Atomic Resolution γ-ray Holography Using the Mössbauer Effect

P. Korecki,[1] J. Korecki,[2] and T. Ślęzak[2]
[1]*Institute of Physics, Jagiellonian University, Reymonta 4, 30-059 Kraków, Poland*
[2]*Department of Solid State Physics, Faculty of Physics and Nuclear Techniques, University of Mining and Metallurgy, 30-059 Kraków, Poland*
(Received 10 June 1997)

We have observed a strong (2%) angular modulation of the total backscattered conversion electron yield, measured as a function of the incidence angle of the 14.4 keV γ rays from a ^{57}Co Mössbauer source irradiating thin epitaxial ^{57}Fe film grown on MgO(001). The measured 2D pattern is the first hologram of the local surrounding of the absorbing nuclei obtained due to nuclear resonant scattering of γ rays. The real space holographic reconstruction shows distinct features corresponding to the nearest neighbor sites in the bcc α-Fe structure. [S0031-9007(97)04412-8]

PACS numbers: 76.80.+y, 07.85.–m, 42.40.–i

Holography with atomic resolution involving radiation from internal emitters was proposed by Szöke [1] and it was applied in the last decade for direct imaging of surfaces, mainly using low-energy electrons [2–9]. Recently Tegze and Faigel [10] first discussed atomic resolution x-ray fluorescence holography (XFH) for bulk crystals. They also suggested to use for holography γ rays which are emitted in resonant recoilless processes from nuclei embedded in a crystal (Mössbauer effect) [10,11]. A photon emitted in such a process may reach a far-field detector directly (holographic reference wave) or it may be additionally scattered from closely situated nuclei (object wave). The interference of the two waves gives a single hologram. The unique total holographic pattern is formed if all emitter neighborhoods are equivalent.

Nuclear resonant scattering is ideally suited for an inner source holography. For the most popular Mössbauer transition 14.4 keV in ^{57}Fe the wavelength of 0.86 Å allows atomic resolution. On the other hand, for this wavelength the nucleus can be treated as a point scatterer. Consequently, the resonant nuclear scattering is more isotropic [12] than the x-ray Rayleigh electron scattering used for XFH [13]. Finally, the coherent γ scattering is sufficiently strong ($\sigma_{\mathrm{coh}} = 3 \times 10^{-4}$ Å^2 [12]). We have calculated that for a model ^{57}Fe cluster the holographic oscillations should be 3% of the reference wave, compared to 0.1%–0.3% observed in x-ray holograms [10,14]. Note also that the hologram acquisition time scales with the square of the effect. The cross section value is however small enough to justify the neglecting of self-interference effects [15].

In spite of its promising perspectives, a straightforward realization of γ holography, as proposed by Tegze and Faigel [11], is experimentally difficult. A monocrystalline sample of ^{57}Fe (only 2.18% abundance) had to be made into a strong radioactive source by introducing ^{57}Co. Because of the high value of the internal conversion coefficient for the 14.4 keV transition ($\alpha = 8.21$) one needs a few tens mCi strong source to obtain a hologram in a reasonable time (months).

The additional difficulty in γ holography is due to a strong Bragg diffraction obvious for single crystalline samples. Bragg diffraction of γ rays, observed for the first time by Black and Moon [16], is presently in common use for nuclear resonant scattering of synchrotron radiation [17]. For internal sources coherent long-range interference effects manifest themselves as Kossel lines [18], similar to those for x rays. The Kossel line pattern begins to form if the number of scatterers contributing coherently to the pattern is of the order of 5×10^4 [11]. However, because of the high spatial frequencies in Bragg or Kossel features one can try to filter them out numerically [10,11,14].

Mössbauer holography can in fact be done more efficiently by applying the optical reciprocity theorem as generalized for magneto-optical systems [18]. A classical version of this idea was recently applied to x-ray holography by Gog *et al.* [14], who developed XFH into multiple-energy x-ray holography (MEXH). In this method, which can be seen as a time reversal of XFH, the positions of the source and the detector are interchanged. The plane wave from a far-field source reaches an atom in a sample (the microscopic detector of the hologram) directly or after being scattered on neighboring atoms. The measured quantity is the total fluorescence yield. Via the MEXH method x-ray holography may be done using strong synchrotron sources. Elimination of twin images becomes possible by applying a multienergy hologram reconstruction algorithm, as successfully applied previously to electron holography [4,5,7–9].

In a similar way, but without the multiple-energy option, we have performed "inverse" γ-ray Mössbauer holography as shown in Fig. 1(a). A photon from an external γ source can be absorbed in the recoilless resonant process by a nucleus in a crystal or it can be additionally resonantly scattered. The interference of these processes gives holographic oscillations of the total number of deexcitation events measured as a function of the γ-ray incidence angle. Rayleigh electron scattering

 0031-9007/97/79(18)/3518(4)$10.00

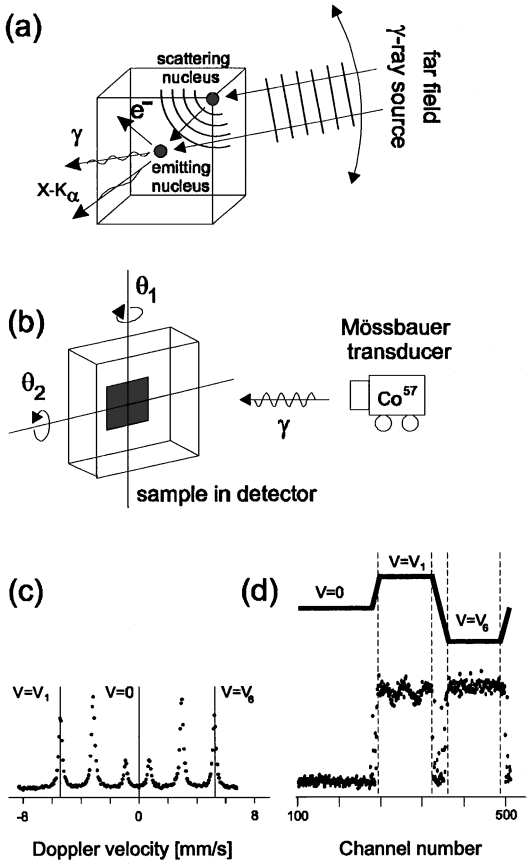

FIG. 1. The basic concept of inverse γ-ray Mössbauer holography. (a) A photon from an external γ-ray source irradiating an ordered sample at variable angle is directly adsorbed by the nucleus or is additionally scattered by nearby nuclei. The hologram is formed due to interference of these processes. The deexcitating nucleus is a microscopic detector of the hologram. (b) Experimental setup. A conventional Mössbauer spectrometer is modified to enable the rotation of the detector (flow proportional electron counter). (c) Conversion electron Mössbauer spectrum of the holographic sample. The velocities used for hologram acquisition are marked. (d) The drive signal fed to transducer moving in the three-constant-velocities mode and the corresponding content of multiscaler channels.

(as in XFH and MEXH) gives also a certain contribution to the hologram (about 20%, as estimated from the comparison of the corresponding cross section values [12]). The possible deexcitation products are reemitted γ rays and products of internal conversion: x rays and electrons. In the case of ^{57}Fe the detection of electrons, 7.3 keV K- and 13.6 keV L-conversion electrons as well as 5.4 keV KLL and 6.2 keV KLM Auger electrons, is the most efficient. The small electron escape depth (2000 Å for inelastically scattered electrons) compared to γ and x rays is compensated by the high value of the internal conversion coefficient and an easy detection over the full solid angle using a proportional flow detector.

The method requiring a single-crystal compound of iron containing only the ^{57}Fe isotope seems to be impractical. Thin epitaxial films which are relatively easy to prepare using molecular-beam epitaxy (MBE) make an exception. Moreover, Mössbauer measurements using conversion electrons are very efficient, permitting us to obtain a spectrum even for a single atomic layer of iron [19].

In our experiment we have used a 2000 Å ^{57}Fe film epitaxially grown by MBE on a polished $10 \times 10 \times 1$ mm^3 MgO(001) single crystal substrate held at 430 K. LEED and x-ray diffraction (XRD) measurements proved that the film consisted of small (001)^{57}Fe crystallites oriented with respect to the MgO substrate in such way that the Fe[100] direction was parallel to MgO[110]. Similarly grown films of natural iron were investigated by us using *in situ* scanning tunneling microscopy. For 200 Å films we observed an island growth with the average diameter of 100 Å. This value coincides well with the broadening of the LEED and XRD peaks observed for our holographic sample. Characterization of our sample by the magneto-optic Kerr effect showed a narrow hysteresis loop of Kerr rotation with the coercive field of 20 Oe and the in-plane easy magnetization axis parallel to [100].

The system described above fulfills ideally the requirements of the holographic experiment. Almost all absorbing nuclei have the same local surrounding, but the long-range periodicity is disturbed by the islandlike structure of the film. This attenuates long-range interference effects and reduces strong but unwanted phenomena such as x-ray Bragg scattering or Kossel lines [19,20].

The sample was placed inside the conventional He/CH_4 filled proportional electron counter [21]. The sample, together with the detector, could be rotated about two perpendicular axes [100] and [010] (lying in the plane of the sample) by angles θ_1 and θ_2, respectively, as shown in Fig. 1(b). This geometry of rotation was chosen because of the expected two-fold pattern symmetry—the measurement was performed in the remanent state, after saturating the film magnetization in the [100] easy direction.

A conventional 100 mCi ^{57}Co(Rh) γ-ray source of 8 mm diameter was moved by a Mössbauer velocity transducer. The sample-detector distance was 15 cm. The transducer was driven in a three-constant-velocity mode. Two of the velocities corresponded to the outermost lines (circularly polarized) of the previously measured Mössbauer spectrum [Fig. 2(c)]. The third one ($v = 0$), corresponding to an off-resonance condition, was used for data normalization. The acquisitions were made separately for each velocity using multiscaler time synchronized with the signal fed to the transducer [Fig. 1(d)]. The total number of counts in channels corresponding to a constant and well defined velocity, normalized to the total of nonresonant counts, was taken as the single pixel value of the pattern. Normalization was necessary to overcome time instabilities of the detection.

The original pattern was recorded on a $d\theta_1 \times d\theta_2 = 1.8° \times 1.8°$ angular mesh in the range from $-43.2°$ to $+43.2°$ for both angles.

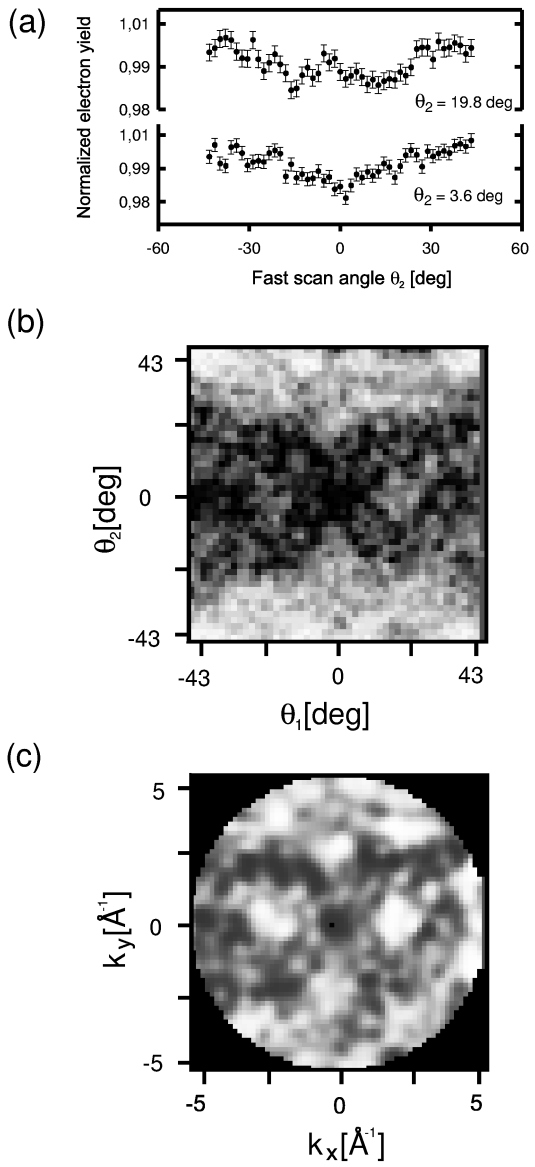

FIG. 2. (a) θ_2 scans of the normalized electron yield obtained for the fixed values of the slow-scan angle θ_1. (b) The full pattern of the normalized scans. (c) The hologram in $\vec{k}$ space obtained from the pattern presented in (a) after background removal and low-pass filtering. The maximum oscillations are about 2%.

Figure 2(a) shows 1D θ_2 scans of the normalized electron yield obtained for a fixed value of the slow-scan angle θ_1. The full pattern of raw (normalized) scans, obtained in about 120 hours, is presented in Fig. 2(b). The number of counts for this pattern is of the order of 5×10^5 per pixel. As expected, holographic oscillations of about 2% are visible. A slowly varying background was derived by Gaussian low-pass convolution as described by Harp *et al.* [22] and then subtracted from the pattern. Additionally, a low-pass Gaussian filter was applied to the resulting pattern in order to eliminate noise. The processed hologram interpolated to a convenient $\vec{k}$ space mesh is presented in Fig. 2(c). The hologram multiplied by an apodizing window function was then reconstructed to a real space using the Helmholz-Kirchoff formula [2]. Two-dimensional slices of the real space reconstruction obtained from the nonsymmetrized hologram are shown in Fig. 3. Slices in the (001) plane parallel and in the (010) plane perpendicular to the film surface, both at a distance of 1.43 Å from the emitter (the interplanar spacing for bcc Fe) are presented in Figs. 3(a) and 3(b), respectively. The positions of the actual atomic crystal sites correspond to the centers of depicted ellipses. The theoretical resolution resulting from the accessible $\vec{k}$ range is reflected in the lengths of their axes. Roughly, the lateral resolution $\Delta x = 0.76$ Å and vertical resolution $\Delta z = 3.12$ Å were calculated according to Ref. [24]. The most intense features of the reconstruction overlap with the nearest neighbors position in α-Fe. A small but visible asymmetry in both the measured pattern and in the holographic reconstruction is caused by strong polarization effects and/or interference between nuclear resonant

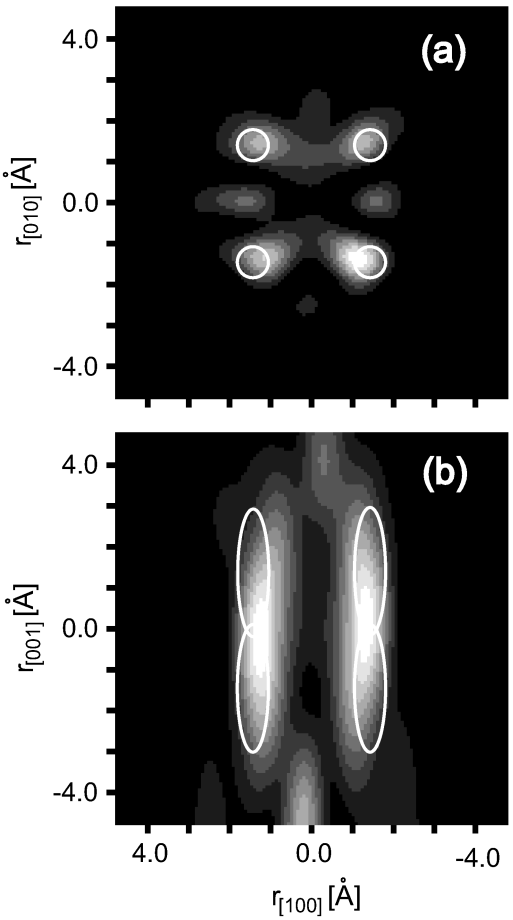

FIG 3. Holographic reconstructions of atomic positions: (a) A (001) cut in a plane 1.43 Å from the emitter. (b) A (010) cut in a plane 1.43 Å from the emitter. The ellipses have dimensions equal to theoretical resolutions in various directions and are centered on atomic sites.

and Rayleigh electronic scattering [12,16,17,24,25]. This is associated with the fact that nuclear transitions in ^{57}Fe are pure M1 and the system is uniformly magnetized. One has also to consider experimental errors in the sample orientation and the asymmetric response function of the detector. All the geometrical uncertainties, including a finite size of the source and a coarse grid used for the acquisition of the hologram, are responsible for small shifts of the predominant features of the holographic reconstruction (positions of nuclei) from the true crystal positions. The holographic reconstruction does not go beyond the first coordination shell. This limitation is mainly caused by the rather poor statistics which in turn forced us to use the low-pass filter, but also by a cancellation of real and twin images. The cancellation may be present in systems with high symmetry. It is caused by a different phase behavior of the real and twin images as a function of the radiation energy used and as a function of the scatterer position relative to the hologram detector (see Refs. [11,13,26]). The modest vertical resolution [compare Fig. 3(b)], additionally deteriorated by the overlapping of the real and twin images, could be improved by modifying the detector to have a higher acceptance angle for incident γ rays. For a full hemisphere the resolution could be better than 0.76 Å in both directions. Other visible features are artifacts due to the aliasing effects arising in the transform, which are difficult to remove because of the low signal-to-noise ratio. Some of the above effects can be easily suppressed by a simple two-fold symmetrization of the hologram.

To summarize, we have presented the first experimental demonstration of a new method for accomplishing atomic resolution holography based on resonant nuclear scattering of γ rays. To record the hologram we have used a conventional Mössbauer experimental setup. By tuning to a particular Mössbauer transition one is able to image individual crystal sites, as determined by a defined set of hyperfine interaction parameters. It should be possible to apply γ-ray holography as a direct visualization tool for crystallographic and magnetic structures of epitaxial layers containing effectively just 100 atomic layers of the ^{57}Fe isotope.

The authors are greatly indebted to Professor Marek Szymoński of the Institute of Physics, Jagiellonian University for inspiration. This work was supported by Polish Science Research Council, Grants No. 2 P03B 080 10 and No. 2 P03B 069 13.

[1] A. Szöke, in *Short Wavelength Coherent Radiation: Generation and Applications*, edited by D. T. Attwood and J. Bokor, AIP Conf. Proc. No. 147 (AIP, New York, 1986).
[2] J. J. Barton, Phys. Rev. Lett. **61**, 1356 (1988).
[3] G. R. Harp, D. K. Saldin, and B. P. Tonner, Phys. Rev. Lett. **65**, 1012 (1990).
[4] J. J. Barton, Phys. Rev. Lett. **67**, 3106 (1991).
[5] S. Y. Tong, Hua Li, and H. Huang, Phys. Rev. Lett. **67**, 3102 (1991).
[6] S. Thevuthasan, R. X. Ynzunza, E. D. Tober, C. S. Fadley, A. P. Kaduwela, and M. A. Van Hove, Phys. Rev. Lett. **70**, 595 (1993).
[7] L. J. Terminello, J. J. Barton, and D. A. Lapiano-Smith, Phys. Rev. Lett. **70**, 599 (1993).
[8] C. M. Wei, S. Y. Tong, H. Wedler, M. A. Mendez, and K. Heinz, Phys. Rev. Lett. **72**, 2434 (1994).
[9] L. S. Caputi, O. Comite, A. Amoddeo, G. Chiarello, S. Scalese, E. Colavita, and L. Papagno, Phys. Rev. Lett. **77**, 1059 (1996).
[10] M. Tegze and G. Faigel, Nature (London) **380**, 49 (1996).
[11] M. Tegze and G. Faigel, Europhys. Lett. **16**, 41 (1991).
[12] J. P. Hannon and G. T. Trammel, Phys. Rev. **169**, 315 (1968); Phys. Rev. **186**, 306 (1969).
[13] P. M. Len, S. Thevuthasan, C. S. Fadley, A. P. Kaduwela, and M. A. Van Hove, Phys. Rev. B **50**, 11 275 (1994).
[14] T. Gog, P. M. Len, G. Materlik, D. Bahr, C. S. Fadley, and C. Sanchez-Hanke, Phys. Rev. Lett. **76**, 3132 (1996).
[15] S. Thevuthasan, G. S. German, A. P. Kaduwela, R. S. Saiki, Y. J. Kim, W. Niemczura, M. Burger, and C. S. Fadley, Phys. Rev. Lett. **67**, 469 (1991).
[16] P. I. Black and P. B. Moon, Nature (London) **188**, 481 (1960).
[17] G. V. Smirnov, Hyperfine Interact. **97/98**, 551 (1996); R. Rüffer and A. I. Chumakov, Hyperfine Interact. **97/98**, 589 (1996).
[18] J. P. Hannon, N. J. Carron, and G. T. Trammell, Phys. Rev. B **9**, 2791 (1974); **9**, 2811 (1974).
[19] J. Korecki and U. Gradmann, Phys. Rev. Lett. **55**, 2491 (1985).
[20] T. Gog, D. Bahr, and G. Materlik, Phys. Rev. B **51**, 6761 (1995).
[21] K. R. Swanson and J. J. Spijkerman, J. Appl. Phys. **41**, 3155 (1970).
[22] G. R. Harp, D. K. Saldin, X. Chen, Z.-L. Han, and B. P. Tonner, J. Electron Spectrosc. Relat. Phenom. **57**, 331 (1991).
[23] J. J. Barton, J. Electron Spectrosc. Relat. Phenom. **51**, 37 (1995).
[24] L. Y. Clark and C. D. Goodman, Phys. Rev. C **6**, 836 (1972).
[25] P. M. Len, T. Gog, D. Novikov, R. A. Eisenhower, G. Materlik, and C. S. Fadley, Phys. Rev. B **56**, 1529 (1997).
[26] P. M. Len, T. Gog, C. S. Fadley, and G. Materlik, Phys. Rev. B **55**, R3332 (1997).